4-3-2019

An Optimization Approach Based on the Interior-Point Methodology for the Tertiary Control of Modernized Microgrids

Isaiah D. Woodruff
Georgia Southern University

2019

An Optimization Approach Based on the Interior-Point Methodology for the Tertiary Control of Modernized Microgrids

Isaiah Woodruff
Georgia Southern University

An Optimization Approach Based on the Interior-Point Methodology for the Tertiary Control of Modernized Microgrids

An Honors Thesis submitted in partial fulfillment of the requirements for Honors in Electrical Engineering

By
Isaiah Woodruff

Under the mentorship of Dr. Masoud Davari

ABSTRACT

With the rise in popularity of the modernized microgrids (MMGs), the addition of a controller to maximize economic efficiency while considering environmental impact is crucial. Tertiary control is at the highest control level, considering economic concerns related to the optimal operation of the microgrid and using a sampling time from minutes to hours; tertiary controls manage the flow of power between the microgrid and the connected grid. In MMGs' tertiary controls, the use of optimization algorithms to minimize an objective function with equality and inequality constraints allows for powerful control over the system. In this paper, the interior-point algorithm is proposed and utilized in order to minimize the required objective. The suggested method is robust against weather conditions and accommodates varying demands in both ac and dc grids. To perform optimization and simulations, MATLAB outputs a lookup table, which can be easily implemented into any system. This is a 2-dimensional array with ac load requirements on the rows and dc load requirements on the columns. Furthermore, due to load capabilities, where the resolution of the system gets too fine, simple algebra can fill in the missing information. Visualization of these results is key to understand what MMG's devices would output for a certain load.

Thesis Mentor: _____

Dr. Masoud Davari

Honors Director: _____

Dr. Steven Engel

April 2019
Electrical Engineering
University Honors Program
Georgia Southern University

ACKNOWLEDGMENTS

I would like to thank Georgia Southern University's Department of Electrical and Computer Engineering for giving me the opportunity to complete this Thesis.

Without the support that I have had along the way from my Mentor, Dr. Masoud Davari, and Dr. Mohammad Ahad—the professor who recommended me for the Honors Program—I would have not been able to have such a great opportunity.

I would also like to say a big thank you to my parents and bother, Martha, Robert and Nathan Woodruff for always supporting my ideas.

This thesis is an original work by Isaiah D. Woodruff. This thesis has been submitted for publication as scholarly articles in which Dr. Masoud Davari was the supervisory author and has contributed to concepts formations and the manuscript composition.

Last, but by no means least, this work has been supported by the U.S. National Science Foundation (NSF) grant—**award #180827**—provided by the core program of Energy, Power, Control, and Networks (EPCN) in the Division of Electrical, Communications and Cyber Systems (ECCS).

INTRODUCTION

The energy sector has been significantly progressing, moving toward simultaneously integrating power networks and energy storage systems—e.g., battery energy storage systems (BESSs)—embedded in ac/dc grids, also called hybrid multi-terminal ac/dc grids (see [1]–[12] and references therein). In smart grids, the modernized microgrid (MMG) concept brings many benefits to the operation, control, and demand supply within commercial power systems. This means that future MMGs will employ a new trend in their power architecture, suggested as a fully integrated power and energy system (FIPES) in this paper, thanks to the integration of BESSs. Briefly speaking, FIPES has a similar structure to what is employed in traditional microgrids and/or power systems—but it highly integrates energy storage units, e.g., BESSs.

Modernized microgrids (MMGs) are emerging as a feasible option for certain communities—Fig. 1. shows an overview. This is because of the increase in funding for renewables as well as the cost reduction of the power electronic technologies that are heavily utilized by MMGs [13]. These power electronics employed in the BESSs using bidirectional voltage-sourced converters (VSCs). Another advantage of the MMG is benefiting from new battery technologies (e.g., see [2]). The items that make up this MMG are photovoltaics (PV), a wind generator (WG), a bidirectional VSC, a diesel generator (DG), and two BESSs, one for the ac bus and one for the dc bus. The ability to store energy in high quantities is crucial when dealing with sources that give uncertain, non-dispatchable electric power (e.g., renewables). The main culprit for this type of output is the curtailed power of PV. Sampling within the hour can result in a power change because of shade and solar conditions. In addition, obviously, this power source is useless at night [14]. When an

MMG is disconnected from the grid, this is known as island mode. For these simulations, the MMG is being utilized in island mode. With no other outlet besides renewable energy sources, this power system must result in the addition of a DG, which will provide the reliability that renewables lack. This generator should not be responsible for increasing the ability of the system to deal with higher loads.

All of the above-mentioned operation considerations are being handled by the tertiary control of MMGs. MMGs' tertiary control is at the slowest—and the highest—control level. It considers economic concerns associated with the optimal operation of the MMG—at a sampling time from minutes to hours—and simultaneously manages the flow of power within the system. A new optimization approach will be proposed in order to come up with the new needs of MMGs' demands. The proposed method is based on the interior-point algorithm, which is able to output the possible generation of both ac and dc power set points and stipulations. More importantly, the proposed method is also robust against changes in weather conditions, including both wind and solar energies.

MATHMATICAL MODEL

Problem Formulation

The objective function can be found in (1). While the inequality constraints involve simple box constraints—both upper and lower limits—to the power sources outputs, the equality constraints take care of the basic laws of physics that must be followed in order to maintain an ac and dc bus. These equations also take into account the startup time for the DG.

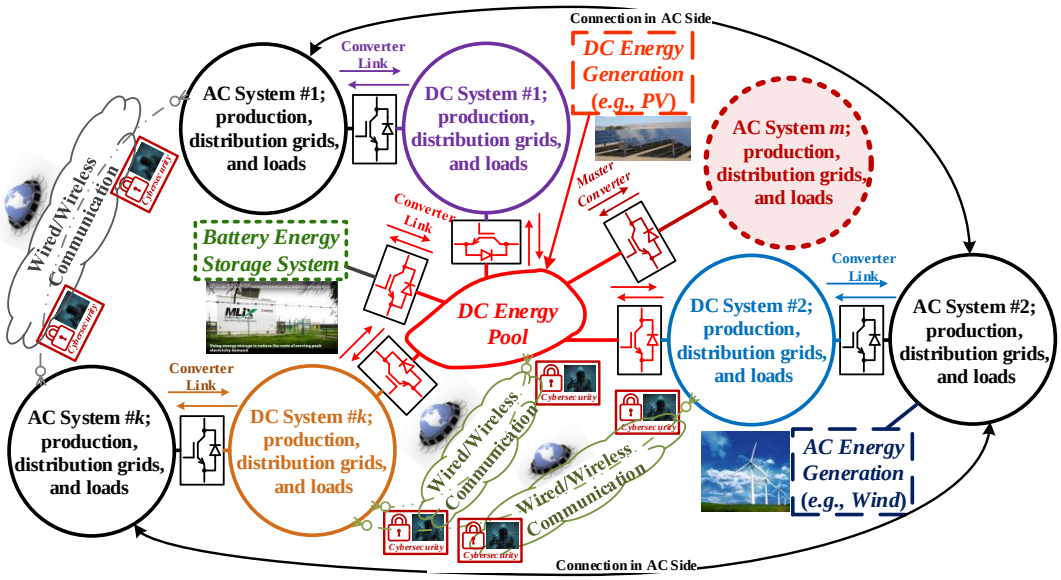

Fig. 1: A notional concept of the MMG

$$\begin{aligned} \min_{p_i} \quad & O.F.(k), \\ \text{s.t.} \quad & g(p) \leq b, \\ & \sum_{i=0}^{n} p_i = 0, \\ & p_j \leq cte, \quad \forall j \in \mathbb{N}, \end{aligned} \tag{1}$$

where

$$\begin{aligned} O.F.(k) = [&\alpha_1 \sigma_{DG}(k) + \alpha_2 P_{DG}^{ref}(k) + \alpha_3 P_{ac\text{-}to\text{-}dc}^{ref}(k) + \\ &\alpha_4 P_{dc\text{-}to\text{-}ac}^{ref}(k) + \alpha_5 P_{BESS}^{ac\text{-}ref}(k) + \\ &\alpha_6 P_{BESS}^{dc\text{-}ref}(k) - \alpha_7 P_{PV}^{ref}(k) - \alpha_8 P_{Wind}^{ref}(k)]. \end{aligned}$$

The equality constraint associated with the FIPES' ac side is given below.

$$\begin{aligned} &P_{DG}^{ref}(k) + P_{Wind}^{ref}(k) + P_{BESS}^{ac\text{-}ref}(k) + P_{dc\text{-}to\text{-}ac}^{ref}(k) = \\ &P_{FIPES'\ Demand}^{ac\text{-}side}(k) + P_{ac\text{-}to\text{-}dc}^{ref}(k). \end{aligned}$$

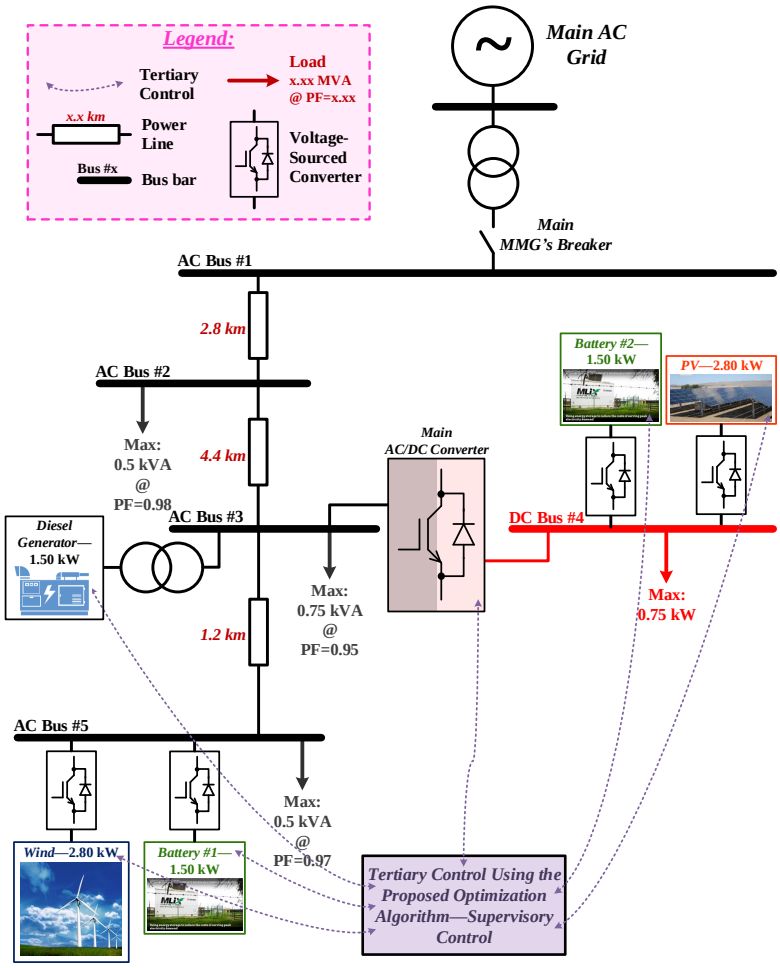

Fig. 2: The simplified CIGRE microgrid used for the studies

The equality constraint associated with the FIPES' dc side is given next.

$$P_{PV}^{ref}(k) + P_{BESS}^{dc\text{-}ref}(k) + P_{ac\text{-}to\text{-}dc}^{ref}(k) =$$

$$P_{FIPES'\ Demand}^{dc\text{-}side}(k) + P_{dc\text{-}to\text{-}ac}^{ref}(k).$$

The inequality constraints associated with the FIPES' ac/dc side are given below.

$$P_{PV}^{min}(k) \leq P_{PV}^{ref}(k) \leq P_{PV}^{max}(k),$$

$$P_{Wind}^{min}(k) \leq P_{Wind}^{ref}(k) \leq P_{Wind}^{max}(k),$$

$$P_{ac\text{-}to\text{-}dc}^{min}(k) \leq P_{ac\text{-}to\text{-}dc}^{ref}(k) \leq P_{ac\text{-}to\text{-}dc}^{max}(k),$$

$$P_{dc\text{-}to\text{-}ac}^{min}(k) \leq P_{dc\text{-}to\text{-}ac}^{ref}(k) \leq P_{dc\text{-}to\text{-}ac}^{max}(k),$$

$$P_{BESS}^{ac\text{-}min}(k) \leq P_{BESS}^{ac\text{-}ref}(k) \leq P_{BESS}^{ac\text{-}max}(k),$$

$$P_{BESS}^{dc\text{-}min}(k) \leq P_{BESS}^{dc\text{-}ref}(k) \leq P_{BESS}^{dc\text{-}max}(k),$$

$$\sigma_{DG}(k)P_{DG}^{min}(k) \leq P_{DG}^{ref}(k) \leq \sigma_{DG}(k)P_{DG}^{max}(k),$$

$$\sigma_{DG}(k-1) - \sigma_{DG}(k-2) \leq \sigma_{DG}(k),$$

$$|P_{BESS}^{ac\text{-}ref}(k) - P_{BESS}^{ac\text{-}ref}(k-1)| \leq \Delta P_{BESS}^{ac\text{-}ref}(k),$$

$$|P_{BESS}^{dc\text{-}ref}(k) - P_{BESS}^{dc\text{-}ref}(k-1)| \leq \Delta P_{BESS}^{dc\text{-}ref}(k).$$

Relevant Optimization Algorithms for the Problem

Objective functions can have many classifications regarding linearity and convexity. The optimization method uses what is known as a trust region to solve many types of optimization problems. A trust region is a set of points in a function where the resulting values can be approximated extremely accurately, and a minimum found. The approximation function is denoted by q [15]. It can be in the user's favor to include a Hessian function for the proposed methodology, as this can greatly reduce the number of iterations before an answer is found [16]–[18]; some examples show a one-third reduction in the number of iterations necessary [19].

Within the trust region, the objective is minimized, via the use of normal iterative methods, with steps being taken in the direction of gradient descent. This direction of descent is calculated using the Newton Raphson method. When an iteration is greater

than the previous iteration, this point is rejected, and the step size is reevaluated. (2) displays a merit function, which is one of the two ways for calculating a new step size. v is simply a scalar value, while $c(x)$ is the constraint violation.

$$merit = f(x) + v \sum \mid c(x) \mid \tag{2}$$

The linear inequality constraints have to do with the maintenance of an ac side and a dc side bus. The powers associated with the components of these buses need to remain equal for the solution to be feasible. Box constraints are included into the problem via the use of categorization. The categories that are possible for this type of constraint involve the open-ended nature of the limits, as well as the gradient of the objective function in the form of a vector with values between the limits of each box constraint being categorized.

Interior-Point Algorithm and Comparison with Dual Simplex Algorithm

The algorithm that has been used to solve this optimization problem is the interior-point algorithm (see [20]–[23] and references therein). While the dual simplex algorithm is the default minimization algorithm for this type of optimizations, the interior point algorithm was able to complete the problem without adjusting the default setting. Later, it was discovered that a change in the constraint tolerance would have led to the dual simplex algorithm's successful completion of the problem. Due to the high volume of data points processed in the time-invariant section of the results, the interior point algorithm performed well to analyze different load demands. With the adjustments made in order to complete the optimization with the dual simplex algorithm, it was slower than the interior point method. This efficiency comes from the addition of so-called "*slack*" variables—

hereinafter denoted by s. This addition creates a general form that is able to take in any equation that is both equality and inequality constrained.

$$\begin{aligned} \min_{x \in \mathbb{R}^n} \quad & f(x) \\ \text{s.t.} \quad & c(x) = 0 \\ & x \geq 0 \end{aligned} \tag{3}$$

While (3) shows the general form of the optimization problem, (4) shows the necessary addition of the slack variables in order to convert an inequality constraint into an equality constraint. This shifts the inequality from being an entire equation to just s—explained above as a "slack variable."

$$\begin{aligned} g(x) - b - s &= 0 \\ h(x) &= 0 \\ s &\geq 0 \end{aligned} \tag{4}$$

Afterward, the algorithm takes the given objective function and modifies it so that the constraints and the objective function combine to make one equation. This is known as an unconstrained nonlinear optimization problem. This function results in a value of infinity when the barrier, where the function is not feasible is reached. Since the objective is to minimize the function, the algorithm will not select these points, because of the fact that any objective function outcome that takes on the addition of infinity could not possibly house a minimum. The way that a constraint is added to the objective function is via the creation of a barrier function shown in (5).

$$\begin{aligned} \min_{x \in \mathbb{R}^n} \quad & f(x) - \mu \sum (ln(x_i) \\ \text{s.t.} \quad & c(x) = 0 \end{aligned} \tag{5}$$

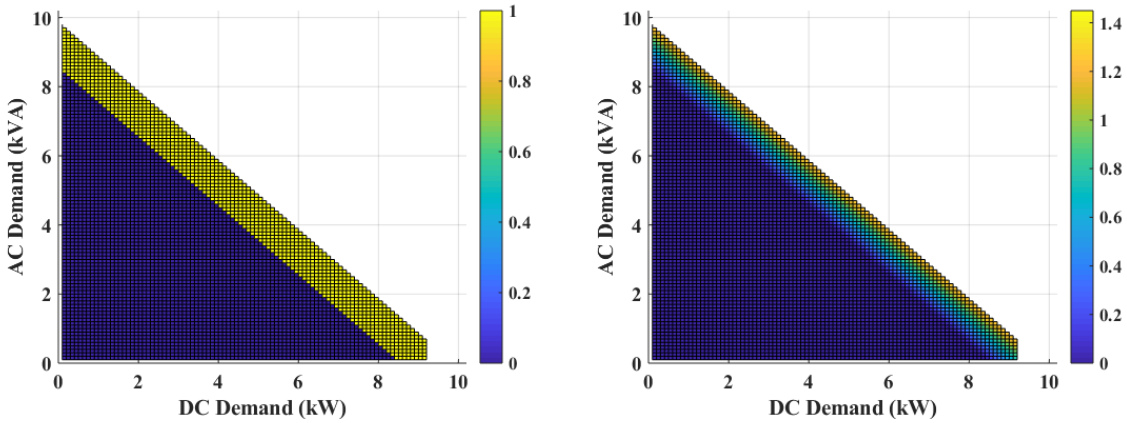

(a) On/Off condition of the diesel generator

(b) Diesel generation

Fig. 3: The outcome of the proposed algorithm for the diesel generator

PROPOSED METHODOLOGY

The objective function that was proposed and considered has in mind economic and environmental benefits. This pursuit of both time-invariant and variant optimization of an MMG started out with the equations that govern such a system. An understanding should be developed on the purpose of each variable, as well as how these variables interact.

Variables

The first variable that is incorporated in the equation is σ. This is an on/off condition of the DG. As it is a common practice in the operation of microgrids [11], the DG is not running all the time. As seen in (1), there is also one sampling time k that σ will be "1," however, the DG power must remain zero as a startup delay is necessary to take into account.

The DG is present to provide reliability. For those few times when there is no wind at midnight—and hence no PV or WG resulting in a worst case scenario—the DG can

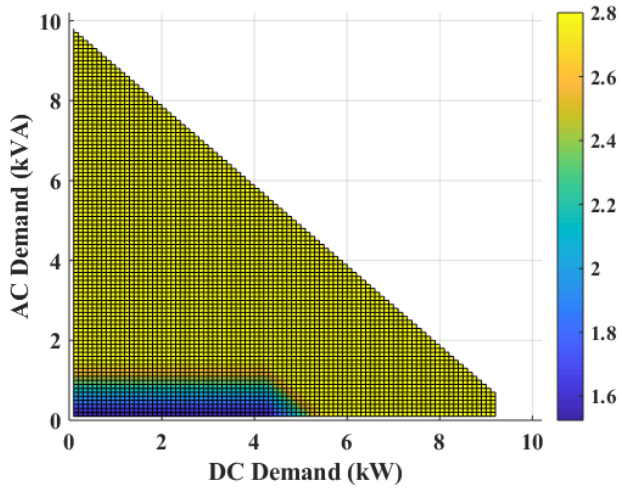

Fig. 4: The outcome of the proposed algorithm for the wind generator

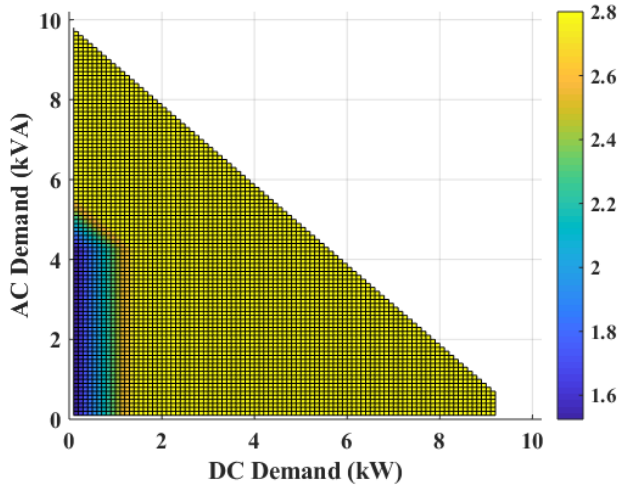

Fig. 5: The outcome of the proposed algorithm for the photovoltaics

come on and provide that little bit of extra power. The addition of the large BESS also allows for the times when the generator is on to be very rare. The use of a variable speed generator is also used to further reduce the impact of this device on the cost and environment. From a coding standpoint, the binary nature of the σ was the most difficult

aspect of the equation to implement. This statement may seem absurd, as binary values are usually the strong suit of computer analysis, however, this type of analysis is not included in the context of the proposed optimization methodology. The solution to this issue was rather straightforward, however. The optimization problem is simply evaluated twice. Once with a value of "0" for σ and then a value of "1." The only scenario where the DG should be turned on is when demand would otherwise be infeasible. Because of the heavy penalty of turning the DG on, this approach leads to the minimum solution. This penalty is better understood by analyzing the values for the coefficients a that multiply by each reference variable in order to give them a weight within the context of the objective. As this is a minimization problem, a higher value of a indicates inefficacy of a device. The value for a of the DG and σ for the DG are ten times that of the conversion variable, the next highest value for a; Fig. 2 shows the simulated MMG—whose parameters are given in Table II.

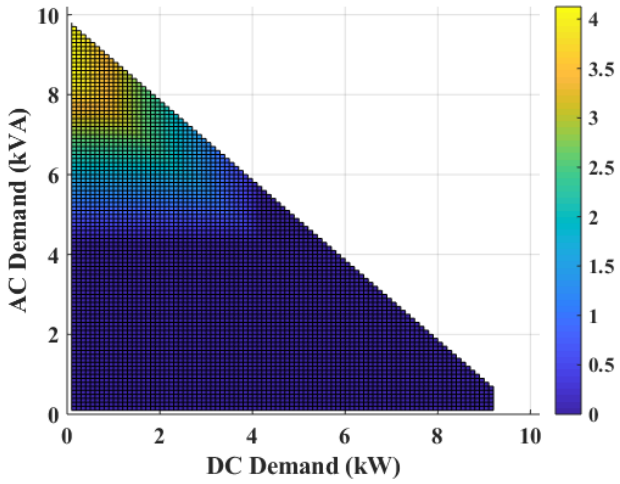

Fig. 6: The outcome of the proposed algorithm for the dc to ac conversion

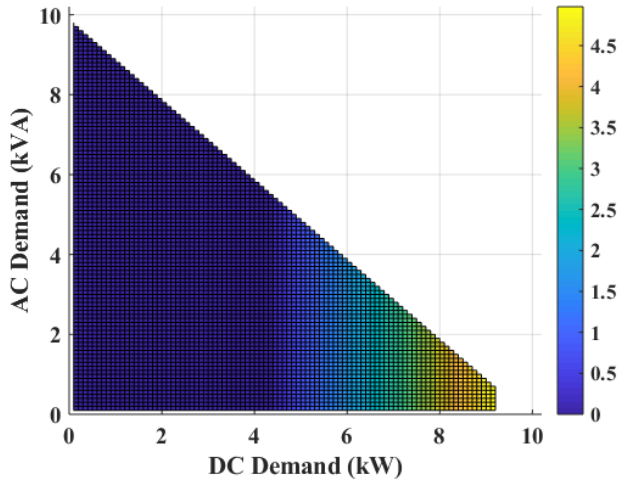

Fig. 7: The outcome of the proposed algorithm for the ac to dc conversion

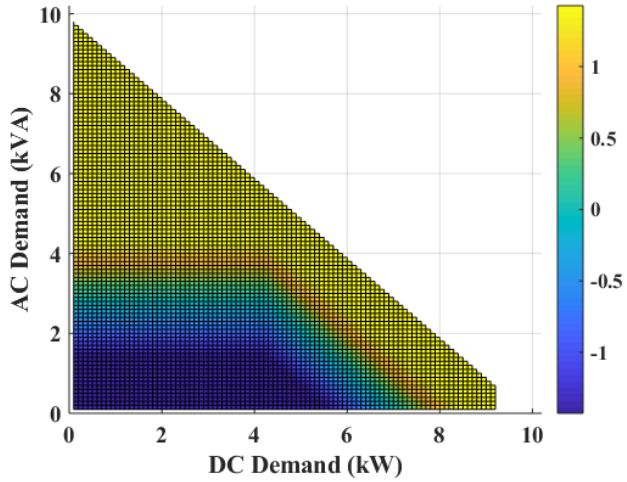

Fig. 8: The outcome of the proposed algorithm for the ac side of the battery energy storage system

Variable Types

The variable type that can change in the objective function is known as the reference. Denoted by P^{ref}, these variables are part of the object that is the optimization prob-

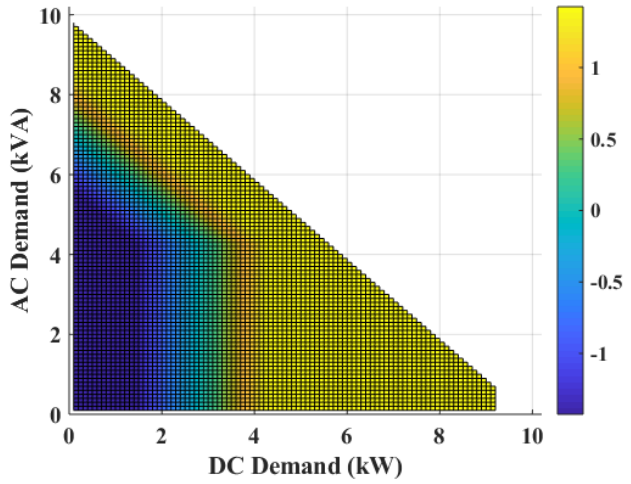

Fig. 9: The outcome of the proposed algorithm for the dc side of the battery energy storage system

lem. These reference variables are stored inside a structure which can be found in the workspace once the code is formulated correctly and run. The objects structure can be turned into a scalar and stored in a matrix. This leads to the ability to create a lookup table from the optimization method's output. These reference variables are constrained by minimum and maximum values that govern their operation given in Table I. For the time-invariant simulation, these values are held constant to understand the interaction of ac and dc demand on the system components. During the time-variant portion of the simulation, these values were allowed to change. For the BESSs, this meant the creation of the state of charge (SOC). The previously used P_{BESS}^{ref} is simply the derivative of this new variable. While the time-invariant system saw demand capabilities of approximately 10 kW, the time-variant system saw a maximum demand capability of around 2.5 kW because of a reduction in the possible power output of the WG and PV systems. While

demands of higher values were possible, certain periods of time would result in blackouts due to various factors. Some of these include weak solar cell performance at night, as well as the sporadic wind conditions. While the demand could vary based on data found in [2], the percentage of the demand for the ac side and the demand for the dc side were held at a constant 70% ac and 30% dc. While normal grid-connected systems would require an overwhelming amount of ac power, future MMGs could improve in the use of dc power that comes from prevalent solar energy, as well as other types of dc-shaped energies. While conversion is an option, there are losses in that transfer of energy and therefore dc devices will continue to be a mainstay in this type of system.

SIMULATION RESULTS

Objective Function

The objective function is flat for the lower ac and dc demands, with the addition of the charging batteries improving upon this value. After that section of the graph, there is a large plateau where the function does not increase greatly. However, once the heavy penalty of the DG is incurred, the objective function jumps. As this objective function is modeling the cost of the system, owners of such a system would want to improve upon other areas before trying to supply a high load that will spike the objective to 2 or more. This is the case when it is necessary to turn the DG on.

Diesel Generator

As stated earlier, the DG is not in place in order to increase the demand capabilities of the system. This increase is marginal and also results in heavy hits to the objective

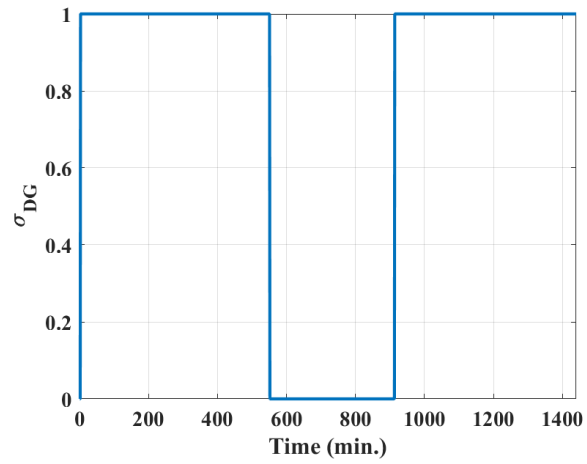

(a) On/Off condition of the diesel generator

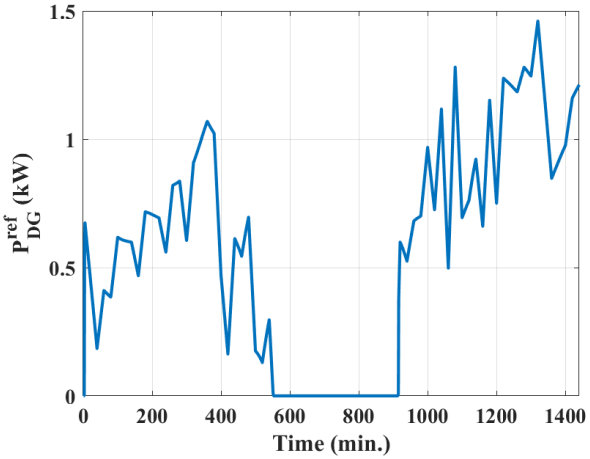

(b) Diesel generation

Fig. 10: The outcome of the proposed algorithm for the diesel generator

function. The importance of using a variable speed generator is also important as the generator only hits peak performance for a select few cases, as can be seen in Fig. 3b and Fig. 10b.

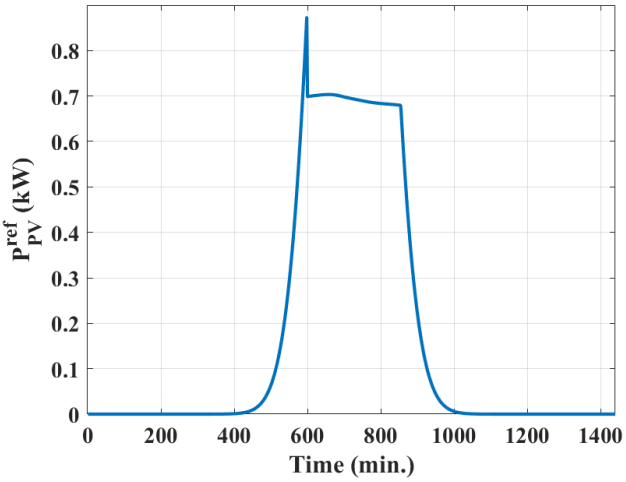

Fig. 11: The outcome of the proposed algorithm for the photovoltaics

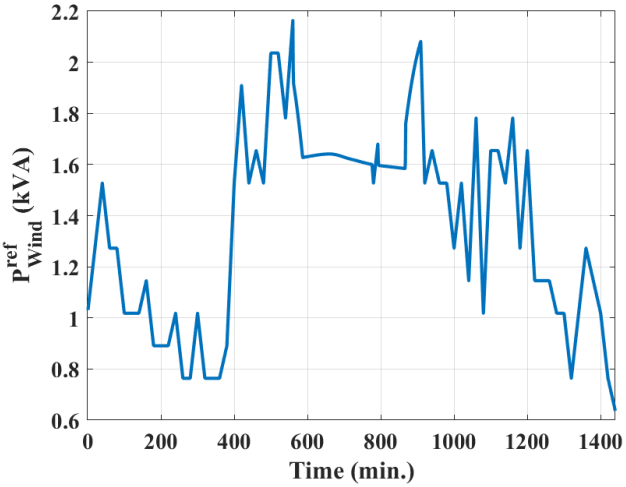

Fig. 12: The outcome of the proposed algorithm for the wind generator

Wind Generation and Photovoltaics

The objective function is accomplishing its goal of emphasizing the use of the “free” energy gathered by the renewable sources. These are the first devices to increase to their

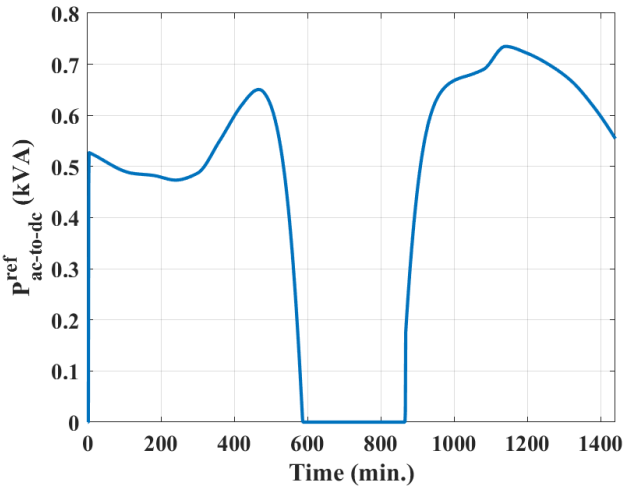

Fig. 13: The outcome of the proposed algorithm for the ac to dc conversion

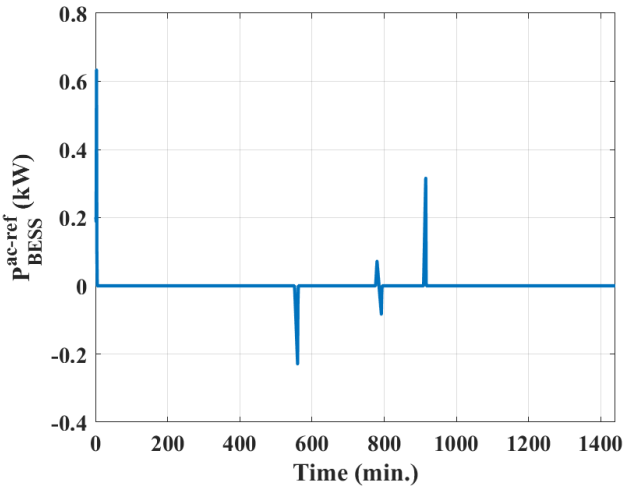

Fig. 14: The outcome of the proposed algorithm for the power of the battery energy storage system—associated with the ac side

maximums, as can be seen in Fig. 4 and Fig. 5. However, there is a slight preference for the wind generator to provide power when dc demand is marginal. To explain this, the solar data that was fed into the system is given by (6) where $f(t)$ is the instantaneous

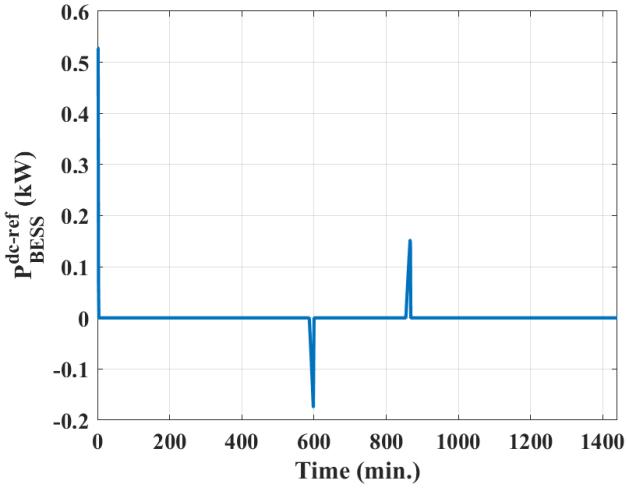

Fig. 15: The outcome of the proposed algorithm for the power of the battery energy storage system #2—associated with the dc side

solar flux density (W/m^2). The graph of this function looks like a bell curve, however, Fig. 11 does not as the algorithm opted to invest in P_{Wind}^{ref}, due to the higher ac demand.

$$f(t) = ae^{(\frac{-b(t-t_0)}{60})^2} \tag{6}$$

b refers to the time it takes for the flux density to ramp up, while a has to do with peak density. The values for these were 261.6 and 0.282 respectively. Finally, t_0 denotes when midday occurred, 720 for this application, with the day broken down into 1440 minutes on the x-axis of Fig. 11. In order to implement the varying output of the WG, wind data from January 9, 2019, near Statesboro, GA was used—just as an example. The wind and solar data have been collected from [24], [25] as referred below.

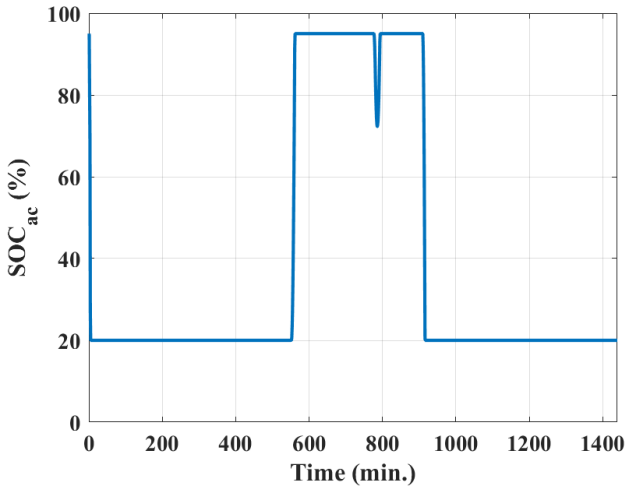

Fig. 16: The outcome of the proposed algorithm for the SOC of battery energy storage system #1—associated with the ac side

Conversion

As can be seen from time-invariant simulation, the feasible solution region is nearly linear, with the ac and dc demand being sustainable if their sum is less than 9.6. There is a small region in the bottom right-hand corner of every graph where the dc demand cannot keep up. This is due to the DG being an ac source. When every device is performing at its maximum power, the converter is not able to accommodate the conversion of the DG, WG, and ac-side BESS (e.g., BESS #1), as the sum of these devices maximum power is 5.8 kVA which is 0.8 kVA more than the ac to dc converter can handle. Finally, in order to clarify, there is no $P^{ref}_{dc\text{-}to\text{-}ac}$ dc to ac counterpart to Fig. 13, because of the heavy ac requirements of the time-variant system. The $P^{ref}_{dc\text{-}to\text{-}ac}$ graph was simply zero for all values of time.

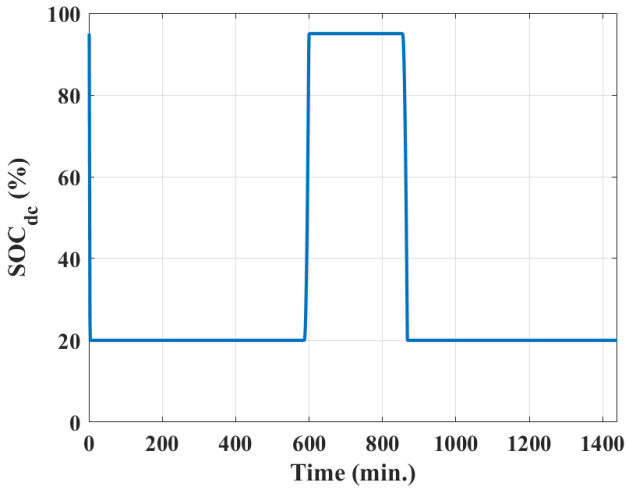

Fig. 17: The outcome of the proposed algorithm for the SOC of battery energy storage system—associated with the dc side

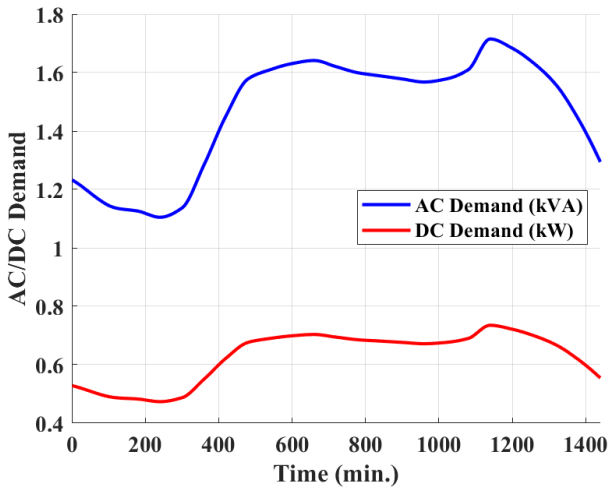

Fig. 18: Demand changes

Batteries

While the battery information from the time-invariant section of the research is not as relevant, the BESSs show their usefulness in the time-variant section of the research.

They are able to jump in when the system is strained, adding to the systems demand capabilities. The real strong suit of the BESS is the ability to help when a large spike in demand occurs. The objective function does not prioritize the charging of the batteries unless the system is well within its demand capabilities.

Time-Variant Simulation

With the variation of the time, the effect of important factors can be visualized. Two of the major real-world factors that were accounted for were wind speed and sunlight intensity. These two factors have a direct correlation with the ability for PV systems and WG output power. In order to implement these factors in the context of the proposed optimization, the task was as simple as manipulating the maximum power of each element. The new solar data was then manipulated in order to create a scalar that varies from 0 to 1 and multiplied by the previous maximum of 2.8 kW—mimicking the curtailed power of PV. The same can be said for the WG.

State of Charge

In addition to the previously discussed sections, the BESSs' state of charge (SOC) variables were also created in the time-variant simulations. This variable was allowed to vary between the values stated in Table I. These values represent 20% and 95% of the maximum charge allowed for the batteries [26]. This is done in order to increase the life of the battery as lithium-ion batteries benefit from this type of constraint. Due to the strange nature of the implementation of the DG in the context of the proposed optimization algorithm, implementing SOC came with some challenges. The issue involved the program losing track of the SOC because of the constant switching on and off of the

generator. In order to combat this, the program looks at the two previous outputs with the same time designation and makes a decision. The program analyzes the problem with an "off" followed by an "on" for σ. If the optimization failed and a feasible solution was not possible, the other solution is chosen. However, the solution that is less likely to fail is also the solution that has the DG on, leading to high objective function value. Therefore, if both solutions are feasible, the solution with the DG off is the final solution.

CONCLUSION

The modernized microgrids' (MMGs') tertiary control, which is considering economic concerns in the optimal operation of a microgrid, has been addressed in this paper. An impactful optimization approach based on interior-point algorithm has been proposed and simulated here. This simulation maximized economical efficiency while taking into account environmental impacts, robustness against weather conditions, and varying ac/dc demands in fully integrated power and energy system (FIPES) of MMGs. The use of the interior-point algorithm minimized an objective function with equality and inequality constraints allowing for meaningful, highly fruitful, tertiary controls over the FIPES. Additionally, due to observed load responses, where the resolution of the system gets too fine, simple algebra can fill in the missing information.

REFERENCES

[1] US Department of Energy, "The War of the Currents: AC vs. DC Power," [Online]. Available: http://energy.gov/articles/war-currents-ac-vs-dc-power.

[2] California Energy Storage Showcase, “Advancing Energy Storage Technology in California,” [Online]. Available: http://www.energy.ca.gov/research/energystorage/tour/.

[3] N. Hingorani, “High voltage DC transmission: A power electronics workhorse,” *IEEE Spectrum*, pp. 63–72, Apr. 1996.

[4] “IEEE application guide for IEEE Std. 1547(TM), IEEE standard for interconnecting distributed resources with electric power systems,” *IEEE Std 1547.2-2008*, pp. 1–217, April 2009.

[5] UL1741 Standard, “Standard for inverters, converters, controllers and interconnection system equipment for use with distributed energy resources,” Jan. 2010.

[6] P. Fairley, “Germany jump-starts the supergrid,” *IEEE Spectrum*, vol. 50, no. 5, pp. 36–41, May 2013.

[7] T. Haileselassie and K. Uhlen, “Power system security in a meshed north sea HVDC grid,” *Proceedings of the IEEE*, vol. 101, no. 4, pp. 978–990, Apr. 2013.

[8] M. Davari and Y. A.-R. I. Mohamed, “Robust multi-objective control of DC-voltage power port in VSC-based hybrid AC/DC micro-grids,” *IEEE Transactions on Smart Grid*, vol. 3, no. 4, pp. 1597–1612, Sep. 2013.

[9] ——, “Robust DC-link voltage control of a full-scale PMSG wind turbine for effective integration in DC grids,” *IEEE Transactions on Power Electronics*, vol. 32, no. 5, pp. 4021–4035, May 2017.

[10] R. Das, V. Madani, and A. P. S. Meliopoulos, “Leveraging smart grid technology and using microgrid as a vehicle to benefit DER integration,” in *Proceedings of the 2017 IEEE Power & Energy Society Innovative Smart Grid Technologies Conference*

(ISGT), Apr. 2017.

[11] J. Shiles, E. Wong, S. Rao, C. Sanden, M. A. Zamani, M. Davari, and F. Katiraei, "Microgrid protection: an overview of protection strategies in North American microgrid projects," in *Proceedings of the IEEE-PES General Meeting*, Jul. 2017.

[12] S. Peyghami, H. Mokhtari, and F. Blaabjerg, "Autonomous power management in LVDC microgrids based on a superimposed frequency droop," *IEEE Transactions on Industrial Electronics*, vol. 33, no. 6, pp. 5341–5350, Jun. 2018.

[13] A. Aghazadeh, N. Khodabakhshi-Javinani, H. Nafisi, M. Davari, and E. Pouresmaeil, "Adapted near-state PWM for dual two-level inverters in order to reduce common-mode voltage and switching losses," *IET Power Electronics*, 2019, *Early Access*— DOI: 10.1049/iet-pel.2018.5268.

[14] R. L. Earle, "Demand elasticity in the california power exchange day-ahead market," *The Electricity Journal*, vol. 13, no. 8, pp. 59–65, Apr. 2000.

[15] M. C. Bartholomew-Biggs, "Algorithms for general constrained nonlinear optimization," *Algorithms for Continuous Optimization*, pp. 169–207, 1994.

[16] J. Nocedal and S. J. Wright, *Numerical Optimization*. Springer, 2006, 2nd Edition.

[17] C. Onwubiko, *Introduction to Engineering Design Optimization*. Prentice Hall, 2000, ch. 4.

[18] A. D. Belegundu and T. R. Chandrupatla, *Optimization Concepts and Applications in Engineering*. Prentice Hall, 1999, ch. 3.

[19] MathWorks, "$fmincon$ Interior-Point Algorithm with Analytic Hessian," [Online].

[20] V. Quintana, G. Torres, and J. Medina-Palomo, "Interior-point methods and their

applications to power systems: a classification of publications and software codes," *IEEE Transactions on Power Systems*, vol. 15, no. 1, pp. 170–176, Feb. 2000.

[21] A. S. Nemirovski and M. J. Todd, "Interior-point methods for optimization," *Acta Numerica*, vol. 17, pp. 191–234, May 2008.

[22] G. Wang, B. Wang, and Q. Fan, "An infeasible primal-dual interior-point algorithm for linearly constrained convex optimization based on a parametric kernel function," in *Proceedings of International Joint Conference on Computational Sciences and Optimization*, Apr. 2009, pp. 900–903.

[23] A. Bitlislioğlu, I. Pejcic, and C. Jones, "Interior point decomposition for multi-agent optimization," *IFAC-PapersOnLine (Elsevier)*, vol. 50, no. 1, pp. 233–238, Jul. 2017.

[24] Z. Guo, "Daily variation law of solar radiation flux density incident on the horizontal surface," *Journal of Astrophysics & Aerospace Technology*, vol. 8, no. 9, pp. 1–5, Aug. 2017.

[25] U. D. of Commerce, "National weather service," 3 Day History, [Online]. Available: https://www.weather.gov/.

[26] M. Hosseinzadeh and F. R. Salmasi, "Robust optimal power management system for a hybrid ac/dc micro-grid," *IEEE Transactions on Sustainable Energy*, vol. 6, no. 3, pp. 675–687, Apr. 2015.

APPENDIX

The Fig. 2's parameters required for the simulation results have been mentioned in Tables I and II.

TABLE I: Inequality Constraints

Variable	Min	Max	Units
σ_{DG}	0	1	Binary
P_{DG}	0.01	1.5	kVA
P_{PV}	0	2.8	kW
P_{WG}	0	2.8	kVA
$P_{BESS}^{dc\text{-}ref}$	-1.125	1.425	kW
$P_{BESS}^{ac\text{-}ref}$	-1.125	1.425	kW
SOC_{dc}	0.3	1.425	kW
SOC_{ac}	0.3	1.425	kW
$P_{ac\text{-}to\text{-}dc}$	0	5	kW/kVA
$P_{dc\text{-}to\text{-}ac}$	0	5	kW/kVA

TABLE II: Objective Function Constants

Constant	Value	Associated Device
a_1	1	σ_{DG}
a_2	1	P_{DG}
a_3	0.1	$P_{ac\text{-}to\text{-}dc}$
a_4	0.1	$P_{dc\text{-}to\text{-}ac}$
a_5	0.01	$P_{BESS}^{dc\text{-}ref}$
a_6	0.01	$P_{BESS}^{ac\text{-}ref}$
a_7	0.0001	P_{PV}
a_8	0.0001	P_{WG}